

Magmatic activity at the NW Hellenic Volcanic Arc (Argolis Peninsula) and its relationship to regional tectonics: An analysis based on 3D aeromagnetic inversion and other geophysical and geological observations.

A. Efstathiou, A. Tzanis and S. Chailas

Department of Geophysics; Faculty of Geology, University of Athens, Panepistimiopoli, Zografou 15784, Greece: aefstathiou@geol.uoa.gr

M. Stamatakis

Department of Economic Geology and Geochemistry; Faculty of Geology, University of Athens, Panepistimiopoli, Zografou 15784, Greece

ABSTRACT

Geophysical methods of analysis were applied in the investigation of the deep structure and geothermal potential of the area, which is related to the Neogene volcanism of the western Hellenic Volcanic Arc (HVA). Herein, we report the results of 3-D aeromagnetic data analysis. The data was inverted with the UBC-GIF magnetic inversion suite, in which geological constraints were applied through several *in-situ* magnetic susceptibility measurements. The results have delineated several isolated (relatively high) susceptibility structures that are no thicker than 300m and have been identified as outcropping ophiolitic bodies. They also indicate the existence of massive deep (ca. 8km) bodies with intermediate susceptibility (0.035 - 0.02 SI), which are attributed to recent magmatic intrusions (plutons). Moreover, detailed images of the local volcanic complex have been recovered at Methana peninsula, including evidence for the magma chamber. The probable presence of the intrusive igneous rocks beneath Argolis peninsula indicates a rather extensive complex of magmatic activity associated with the western volcanic fields of the HVA. In association with seismotectonic observations and geological evidence, it will be argued that this is controlled by the contemporary regional tectonic regime. Finally, it is proposed that the recent plutons and intermediate heat flow density (50-70 mW/m²) of the area also suggest the possibility of geothermal resources in the form of an enhanced geothermal system (hot dry rock).

1. INTRODUCTION

The active south Aegean volcanic arc is considered to be a single arcuate entity stretching from Sousaki at the NW to Nisyros Island at the SE, based on the similar calc-alkaline geochemical environment of all major centers, their Plio-Quaternary age and also the volcanic activity in historical times. Different magma types and their age indicate the presence of two different volcanic groups in the South Aegean volcanic arc (Pe-Piper & Piper, 2005).

The emergence of magmatic material from the upper mantle and through the crust at the NW end of the HVA is clearly imaged in the magnetotelluric section published by Galanopoulos et al (2005). These authors have shown that the structure related to the African and Euro-Asian lithosphere and upper mantle is relatively resistive (>800 Ωm), while the structure associated with the subducting part of the African lithosphere penetrates a relatively conductive (<200 Ωm) asthenosphere with a dip angle of 42°. The area of the western Hellenic Volcanic Arc is clearly imaged with intermediate

electrical resistivities (200–800 Ω m) beneath the Methana – Aegina – Sousaki volcanic centres, as well as beneath the Northern Evoikos Gulf. Argolis Peninsula is located at the western half of the arc where typical calc-alkaline arc-related volcanic rocks of Plio-Pleistocene age predominate and comprises the Methana volcanic complex to the NE. The quaternary volcanic rocks of the Methana Peninsula and the isolated ultrabasic (ultramafic) formations, i.e. (ophiolites, diabases e.t.c.) of the North, Central and South Argolis are expected to yield large magnetic anomalies.

The aim of the study reported here is to investigate the association of these anomalies to the deep structure of Argolis peninsula and the broader magmatic activity of the western ending of the HVA. For this purpose a 3D inversion of aeromagnetic data was conducted. The area was divided into two subregions according to the arrangement of the large magnetic anomalies and surface lithology that were inverted separately, in order to maintain as much detail as possible. The results were interpreted together with seismotectonic observations and provided new information about the deep (crustal) structure of the Argolis Peninsula and the broader western (older) volcanic group of the HVA.

2. GEOLOGY AND REGIONAL TECTONICS

The study area is characterized by complex geological structure comprising Pleio -Pleistocene sediments, ultrabasic formations (ophiolitic mélange), Pre- alpine Upper Paleozoic formations mainly in the southern part (Hydra Island and SW of Astros coastal region) and various alpine series with transition from east interior zones to west exterior zones of Hellenides Specifically Pelagonian Unit with characteristic Jurassic schist chert formation lies on the east part of Argolis peninsula and on the NW part we have small occurrences of calcareous formation of Parnassos Unit as well as flysch of Pindos Unit. A small occurrence of Semimetamorphic Series of Peloponnese – Crete is distinguished on the SWS part of the map (Fig.1).

The volcanism of the area is evident in the presence of the calc-alkaline Methana Volcanic Complex

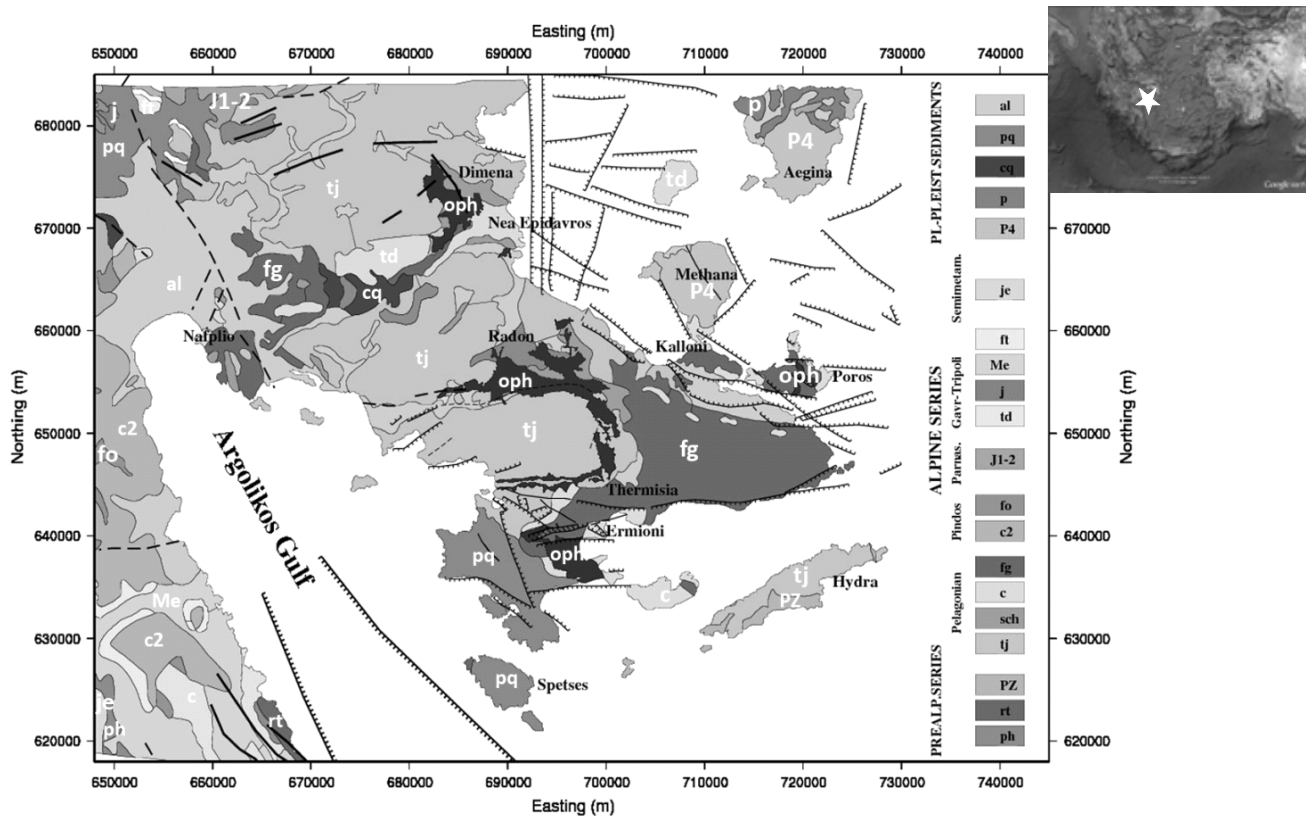


Figure 1: Geographical location of the Argolis Peninsula and geological map.

(MVC) located at the NE coast of Argolis Peninsula with its most recent eruptive episodes at approx. 258 B.C those in Kammeni Chora and at 1700 A.D at the “Pausanias” submarine volcano, NW of Kammeni Chora. Post volcanic activity at the MVC is manifested with geothermal springs at the coastline of Methana peninsula. There is also one thermal spring at the area of Ermioni, with water temperatures $20^{\circ}\text{C} \leq T \leq 40^{\circ}\text{C}$. The heat flow map published by IGME (Taktikos et al, 2001) indicates a high heat flow density (70-150 mW/m²) at Methana Peninsula, an intermediate heat flow density (50-70 mW/m²) at South Argolis, and a relatively low density (30-50 mW/m²) at North and Central Argolis.

The area of Argolis peninsula and Saronikos Gulf are often considered as part of the Corinth Rift system. The Corinth Rift (CR) is a young extensional structure developing in a compressional regime of continental collision and manifesting high complexity and increased seismicity and deformation rates. It is a young basin characterized by E-W normal faulting, with its northern portion lying offshore, below the Gulf of Corinth. Brooks and Ferentinos (1984) portray the Gulf as an asymmetric tectonic basin, a suggestion disputed by Moretti et al, (2003), who consider it to be a symmetric graben. Stefatos et al. (2002) describe it as a composite asymmetric graben, with varying geometry along strike (Sachpazi et al. 2003; McNeill et al. 2005). Geodetic investigations (Billiris et al. 1991; Briole et al. 2000) have shown that the CR is subjected to N-S extension of 1.0 – 1.5 cm/yr. The most recent estimate of the rate of extension at the central CR is approx. 1.1 cm/yr oriented at N185°, while at the western part of the rift it is 1.6 cm/yr at the same direction (De Martini et al, 2004). It is therefore evident that the CR opens up more rapidly in the west than in the east.

Saronikos Gulf lies to the S and SE of the Gulf of Corinth, separated from it by a narrow strip of land known as the Isthmus of Corinth (formed ca. 0.12 Ma ago, e.g. Anastasakis et al, 2005), and the broader Isthmus – Megaris corridor. It is also bounded by the Argolis Peninsula to the W and SW and by Attiki Peninsula to the N and NE. Seismological evidence by Drakatos et al (2005) indicate that Saronikos is divided in two parts by a central platform which, they conjecture, is the offshore

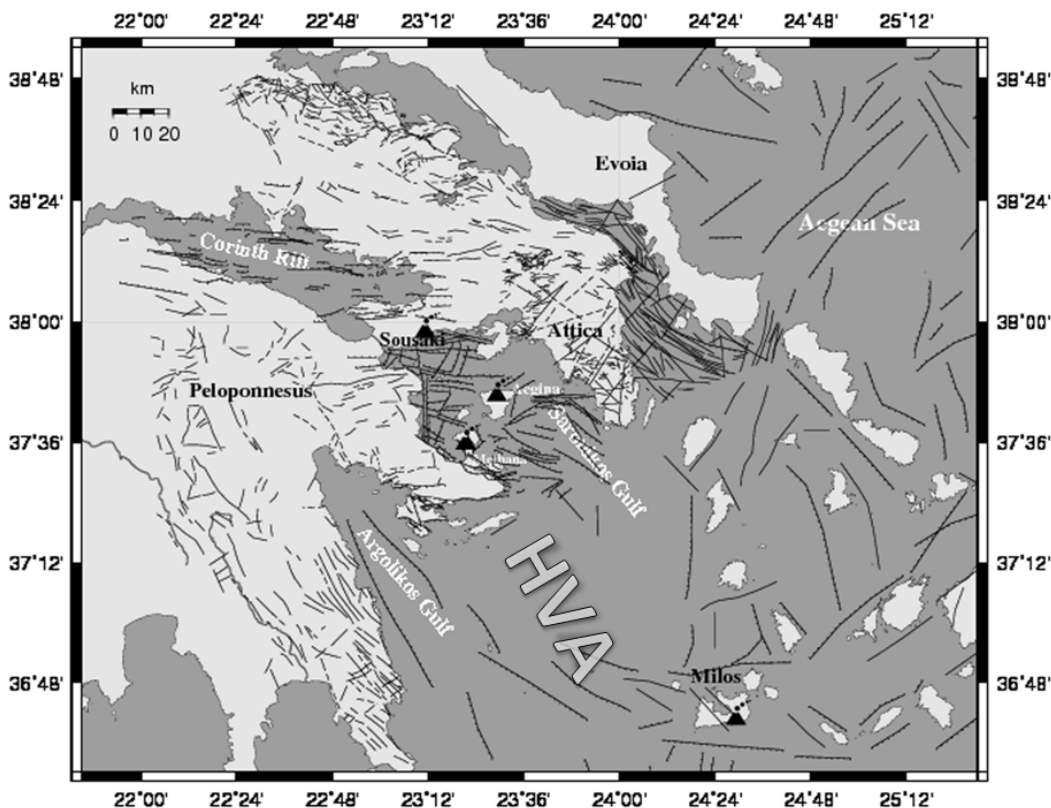


Figure 2: Synthetic seismotectonic map of the western part of the HVA.

extension of a large thrust belt dominating the adjacent onshore areas of Attica. Due to their different structure, the east and west basins are characterized by different seismic velocity values in comparison to the central platform. The western part is characterized by higher seismic activity than the eastern one. Furthermore, the western Saronikos Gulf is divided into a northern and a southern part by a well defined E-W rupture zone, which they interpret this to be an extension of the Corinth Rift fault zone. The same authors assert that crustal thickness is limited to 20 km and attribute their observation to the extensional thinning and the emergence of the mantle material which clearly appears at the depth of 12 km (also see Galanopoulos et al, 2005).

A long line of observational evidence suggests that the expression of normal faulting changes from E-W at the Corinth Rift to WNW-ESE at Saronikos (approx. N110° on average, Papanikolaou et al., 1988) and to NW-SE at the Cyclades (S. Aegean) in two discrete steps (e.g. Papanikolaou and Lozios, 1990, 1991). Additional, and apparently significant faulting structures mapped in Saronikos Gulf, include directions N50°, and N340° (Papanikolaou et al, 1988). The above tectonic information as well as analysis of earthquake focal mechanisms (Ritsema 1974, Hatzfeld et al, 1993) suggest that the contemporary stress field at the Argolikos – Saronikos area is extensional and has NNE-SSW orientation (Kiratzi and Louvari, 2003).

A defining deep dynamic feature of the study area, and one with profound influence on crustal dynamics and the evolution of rapidly deforming extensional structures like the Corinth Rift and the Saronikos Gulf, is the local geometry and dynamics of the African oceanic crust subducting beneath the Aegean plate. Locally, the subducting slab has a NNW strike and ENE plunge, with the dip angle changing rapidly (steepening) approx. beneath Argolis as evidenced by deep earthquake data (Hatzfeld et al, 1989; Suckale et al, 2009; Rontogianni et al, 2011). The sub- crustal stress field is suggested to be extensional and NE-SW due to the aforementioned change in the plunge of the slab (e.g. Rontogianni et al, 2011).

4. AEROMAGNETIC DATA ANALYSIS

4.1 Aeromagnetic maps

The present study utilized an extensive aeromagnetic data set obtained by Hunting Geology and Geophysics Ltd in 1977 under contract by the Institute of Geological and Mining Exploration (IGME) of Greece. The end product was in 1:50000 scale contour maps compiled so, as to comply with the corresponding topographic maps of the Hellenic Army Geographical Survey (HAGS) and the 1:50000 geological maps of IGME. These maps were digitized and recompiled into a unified regional aeromagnetic map of our study area. The image coordinates were transformed to Cartesian coordinates in the UTM system. Finally it was decided to refer the map to an elevation above the highest topographic point at 1100m AMSL (Chailas et al 2010) in order to maintain the data in a compatible form to the inversion suite (Fig.3). Moreover, a set of in situ magnetic susceptibility measurements was conducted in volcanic rocks of the Methana volcanic complex and ultramafic rocks of Argolis peninsula to be used for interpretation.

4.2 3D inversion of the aeromagnetic data

Herein we implement the 3D magnetic inversion algorithms of the University of British Columbia-Geophysical Inversion Facility (Li and Oldenburg, 1996, 1998). This method was chosen for two reasons. Firstly it is flexible in including diverse surface geological information, which may severely constrain the number of acceptable alternative solutions (models), even in the absence of additional deep structural information (as in our case). Secondly, it assumes that the remanent magnetization is negligible and the magnetic response is entirely due to the induced magnetization, avoiding this way complications in magnetic inversion caused by geological and thermochemical processes (Li and Oldenburg, 1996, 1998).

The UBC-GIF inversion program is provided only for Windows OS. Memory limitations in such

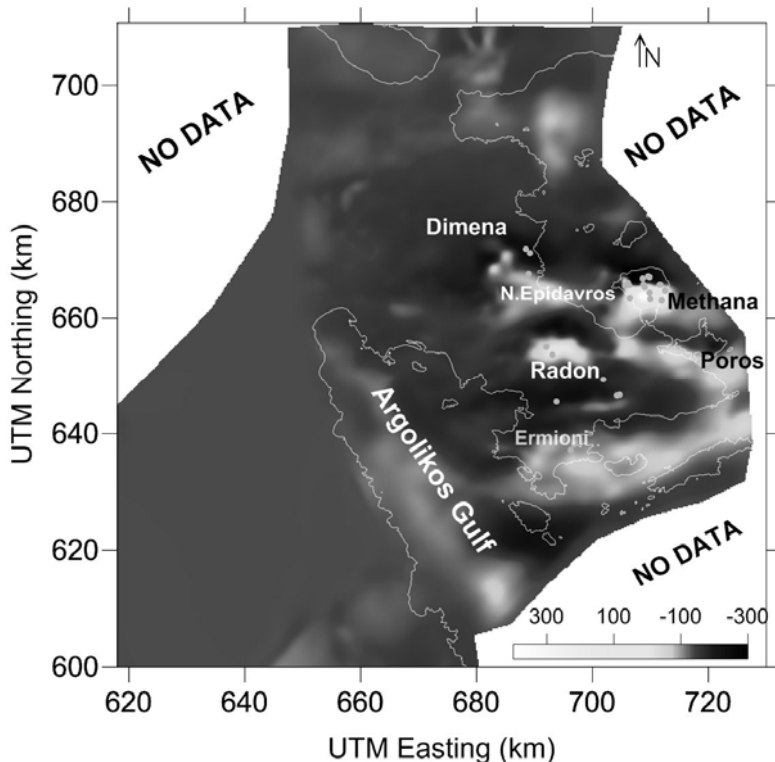


Figure 3: The unified magnetic anomaly map upwarded at 1100m above the mean sea level. The light grey circles indicate the sites of magnetic susceptibility measurements.

systems render impossible the inversion of the entire aeromagnetic data set at once and at the desired level of detail. In consequence, the study area was divided into a northern and southern sub-regions based on the arrangement of aero magnetic anomalies and the available geological information. For each subregion the input data comprised the grid of total field intensities, the topography (Digital Elevation Model with grid size and spacing identical to that of the aeromagnetic data) and the discretized model of Earth structure, (mesh). The mesh was defined on a right rectangular coordinate system and comprised a three-dimensional array of right rectangular prism cells (Fig.4 top). The maximum depth of the mesh was large enough as to ensure that there cannot be magnetic materials below that depth, such that would produce a noticeable anomaly of scale comparable to the scale of the area covered by the data and, therefore, irresolvable discrepancy between the data and the model produced by the inversion.

In order to guide the inversion and constrain the model, all the available information about the structure of the study area has to be considered; this includes surface geological information, borehole data, structural information from geophysical cross-sections etc. In our case, the only available information was surface geological information i.e. lithology and in situ magnetic susceptibility measurements. Based on this information, variation bounds and an initial model for the inversion have been constructed (Fig.4 bottom). The lower bound comprised the lowest susceptibility measured in a given lithological or petrological unit. Conversely, the upper bound comprised the highest susceptibility measured in the same unit. Mesh cells within a given geological formation were assigned with the upper and lower bounds determined for the formation.

Due to the absence of information from the deep geological structure, as was mentioned above, this assignment was limited to cells within the top 250 – 500 m of the mesh (superficial constraints only). The remaining (deeper) cells were allowed to vary in the range of $[0+, 1]$, since the susceptibility of naturally occurring materials is positive and we also need to impose the constraint that all model elements are also positive. In this way each cell of the mesh corresponding to a known and palpable geological formation was characterized by a unique range of susceptibilities with the highest values representing the upper bounds and the lower values the lower bounds.

4.3 Results

At the northern sub-region (North and Central Argolis), the observations are reproduced to within the nominal observational error, rendering the solution “very good”. As can be seen in Figure 5 the model reproduces the observation to better than 5%, with the exception of the central Methana area, where the error locally rises to 17.33% generating a maximum residual of < 99 nT around the peak of the main magnetic anomaly. This considerably high error is due to the coarse discretization (and consequent low resolution) of the model at the specific area. By refining the discretization, this large residual disappears (e.g. Efstathiou et al, 2012); this proves that it is indeed a local artifact of the model.

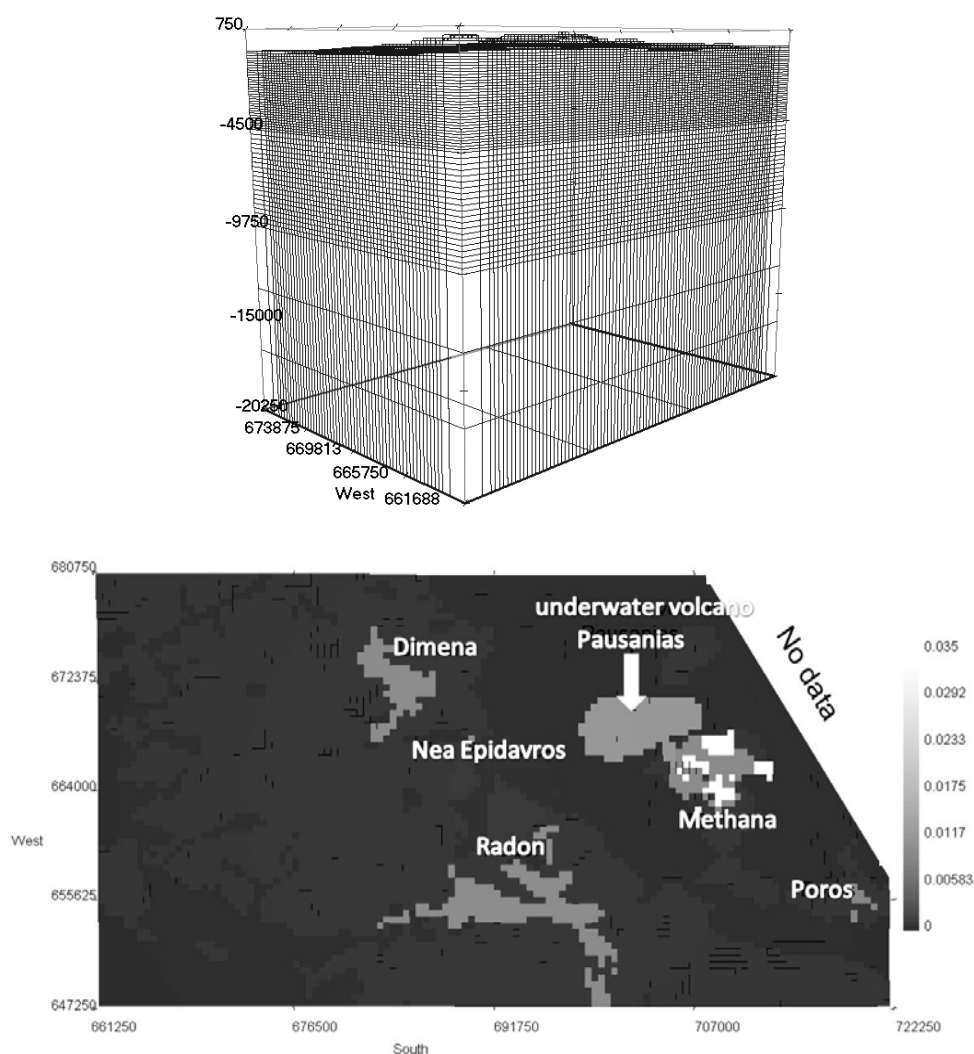


Figure 4: **Top**, Illustration of the mesh, **Bottom**: plan view of the initial model for the northern sub-region. Different shading corresponds to different magnetic susceptibility values of surface geological formations.

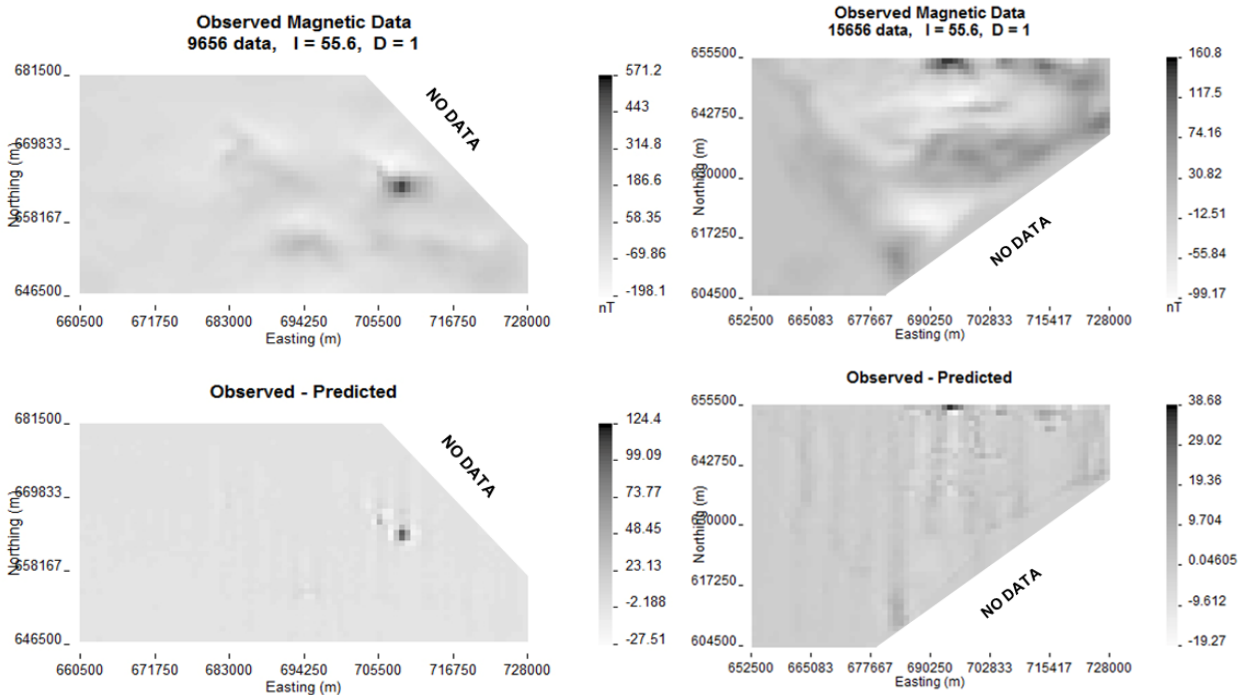


Figure 5: (**top left**) Map of the observed aeromagnetic anomaly at North and Central Argolis; (**bottom left**) the residuals of the observed minus the theoretical anomaly computed for North and Central Argolis; (**top right**) Map of the observed aeromagnetic anomaly at Southern Argolis; (**bottom right**) the residuals of the observed minus the theoretical anomaly computed for South Argolis.

At the southern subregion, (Fig.5) the model reproduces the observation to better than 4%, with the exception of a limited area around Radon, at the central-north sector of the area, where it locally rises to 24.5% generating residuals of the order of 38.68 nT. This, in fact, was expected because the negative lobe of the anomaly due to the Radon ophiolites was not included in the inversion, thus resulting in locally incomplete imaging and poor resolution. A additional source of misfit may be the the existence of a small remanent magnetization in the Radon ophiolites that was not assigned during the inversion.

5. INTERPRETATION

The magnetic susceptibility models will be discussed on the basis of isometric surfaces (isosurfaces). An isosurface will always comprise a 3-D shell of equal susceptibility (k) values enclosing all the k values that are greater than the value of the shell. Susceptibility values less than the value of the isosurface are not shown at all (empty space). In the case where a given isosurface value happens to enclose a domain of lower susceptibility values, then the isosurface is constructed to comprise a convex hull. In all cases, the artifacts produced on the mesh boundaries were eliminated or suppressed.

At North and Central Argolis Peninsula and for susceptibilities of the order of 0.04 - 0.035 the model turns up with large magnetized domains beneath the area of Dimena, Radon and N. Epidavros and some smaller bodies at Poros Island (Fig.6a). These correspond to the large magnetic anomalies related to the ophiolitic formations outcropping at the above areas. As can be seen in the S-N section of Figure 7b, these domains do not exceed the depth of 2km depth and they also dip to the NNE, a trait suggesting that they have been tectonically emplaced (also see Gaitanakis & Photiades, 1989). By decreasing the susceptibility value at 0.025 a body buried at depths greater than 4km can be seen, almost beneath the coast of Nea Epidavros; this corresponds to the significant magnetic anomaly observed at that area and extends to approx. 8.5 km depth (Fig. 6b). The differences in the

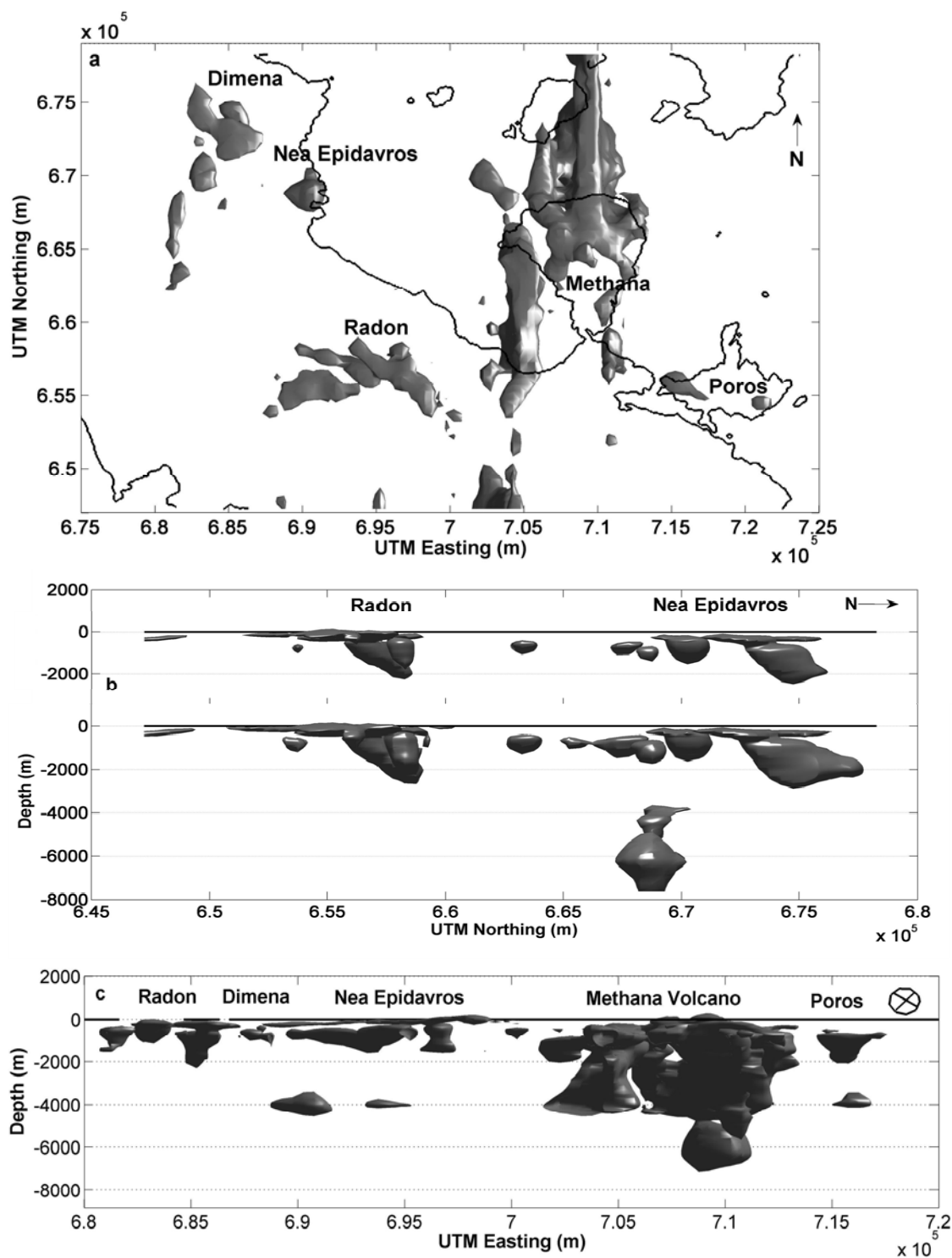


Figure 6: The susceptibility model of North and Central Argolis peninsula; (a) outline of magnetic bodies with magnetic susceptibilities $k \geq 0.035$ SI; (b) S-N cross sections of the model at $k = 0.035$ SI and $k = 0.03-0.02$ SI; (c) E-W cross section of the broader area of North and Central Argolis Peninsula at $k = 0.035$ SI.

susceptibility, placement and geometry of this body with respect to the ophiolites indicate that this particular structure may be due to a different petrological formation.

The differences in the surface lithology between the volcanic domain of Methana and the rest of Argolis peninsula are also reflected in the susceptibility structure. As can be seen in the E-W cross section of Figure 6c, the massive bodies corresponding to the Methana volcanic complex extend to a

depth of 4 km with evidence about the presence of a more weakly magnetized domain at depths up to 7 km (Efstathiou et al, 2012). The susceptibility values of this domain are consistent with the values expected for hot calc-alkaline igneous rocks (200°C – 500°C), so it is interpreted to comprise a magma chamber. In addition to temperature, another argument that this feature is indeed a magma chamber stems from the comparison of magma chambers' depths beneath continental volcanoes (Scaillet et al, 2008; Nomikou & Papanikolaou, 2010).

At the southern sub-region (South Argolis Peninsula), a relatively large and well defined magnetic body has been clearly identified in the area of Ermioni, in addition to a number of smaller structures aligned in a W-E and S-N direction, to the east and north of the Iliokastro and Thermisia regions (Fig.7a). The geological counterparts of these structures are ophiolites and, as can be seen in the S-N cross section of Figure 7b, they comprise lenses which do not exceed the depth of 300 m.

The iso-k surface of 0.02 SI (Fig.8a) indicates the existence of massive magnetized bodies at Ermioni and Thermisia – Iliokastro region. In addition, a massive magnetized domain is detected along the axis of Argolikos Gulf, extending in a SE-NW direction. Because of incomplete imaging below the northing of 620000 m, this large body cannot be completely resolved albeit it is clearly related to the large magnetic anomaly which is present at that area. As can be seen in Figure 8b these massive domains reach 8 km depth. It is apparent that two different geological formations are present. The higher (>0.035 SI) susceptibility formations are no deeper than 300 m and are ophiolitic in composition. The lower ($k < 0.025$ SI) susceptibility domains are massive and present at considerable depths. These features (depth and iso-k value) are comparable to those of the weakly magnetized domain beneath Methana Peninsula that was interpreted as magma chamber. For this reason these massive structures beneath Argolis Peninsula represent recent magmatic intrusions (plutons).

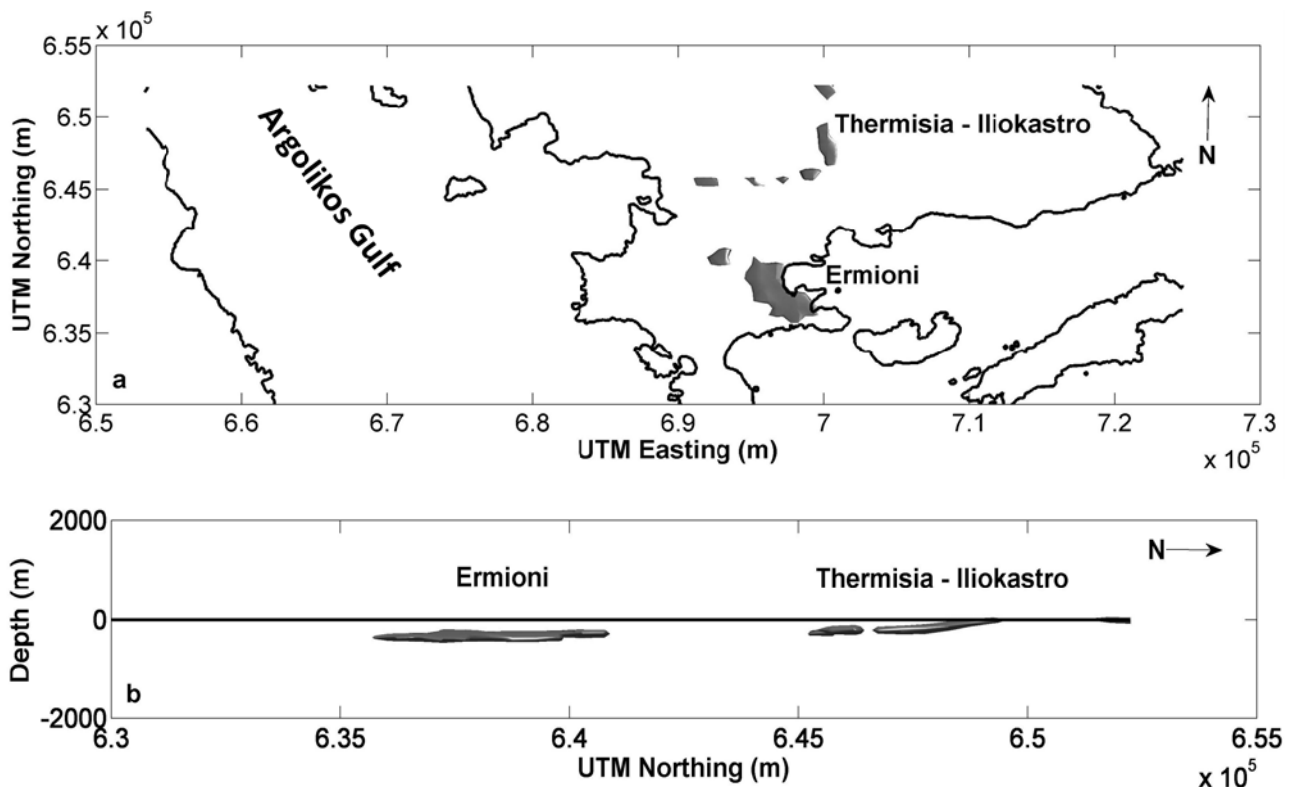


Figure 7: The susceptibility model of South Argolis peninsula; (a) Orthographic projection of the 0.035 isosurface viewed from above; (b) S-N section of the 0.035 isosurface viewed from the East;

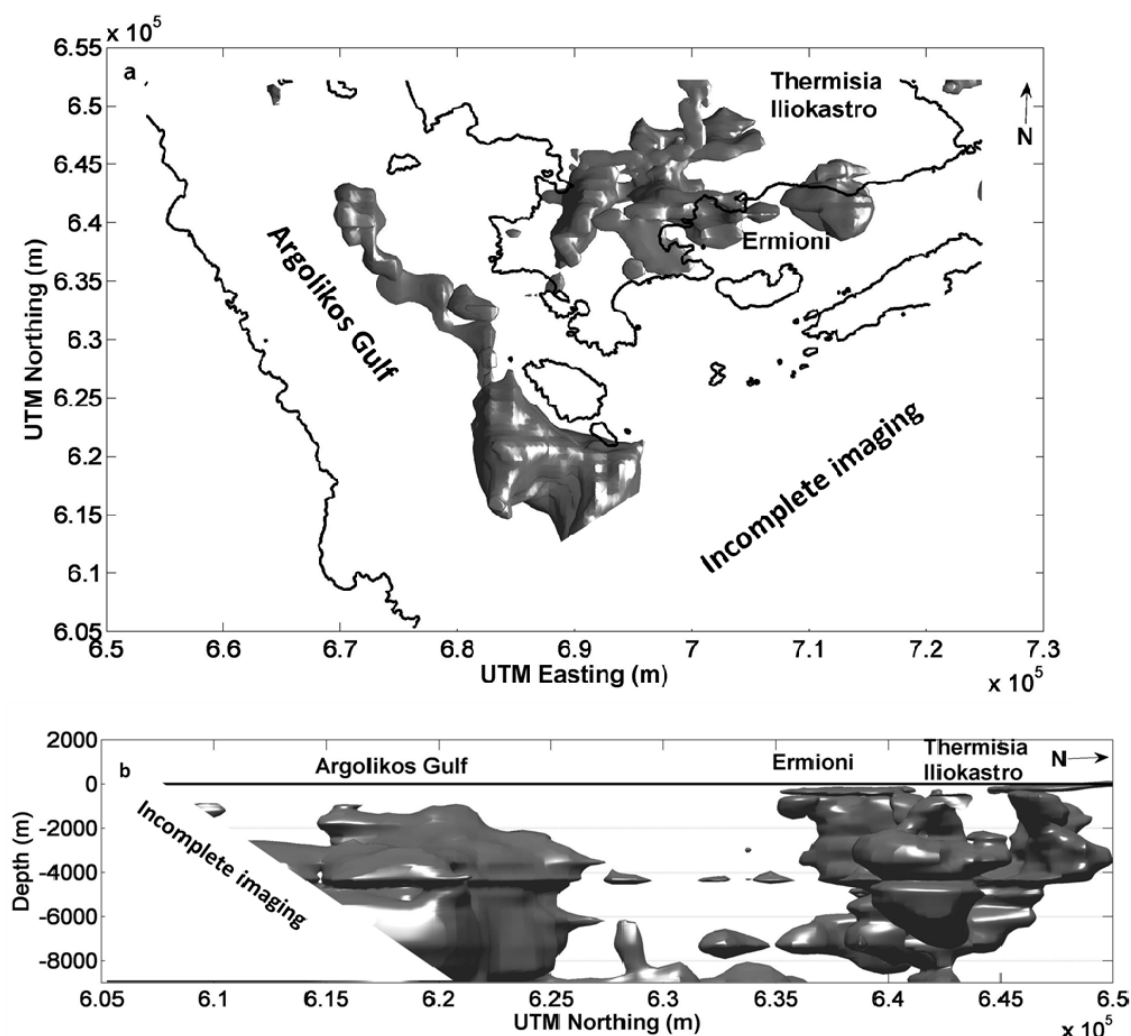


Figure 8: The susceptibility model of South Argolis peninsula: (a) Orthographic projection of the k 0.02 isosurface viewed from above; (b) SW-NE section 0.02 iso- k surface viewed from the East.

In Figure 9 we illustrate the domains that seem to correspond to the magmatic activity of the area. As can be seen magmatism develops in association with significant faulting zones. In the case of Methana Peninsula the emplacement of volcanics seems to be controlled by the tectonics and in particular by faults of NW-SE and NE-SW direction that might have helped the molten material to upwell to the surface. An elongated significant domain of N-S direction is present off the west coast of Methana and has a clear continuity to the South Argolis while in Argolikos Gulf a NW-SE domain is evident and seems to correspond to large faults of the same direction. Significant changes of the stress field between the Corinth Rift and Argo-Saronikos Gulf allow the presence of faults of horizontal E-W direction in which the domains beneath Ermioni and Thermisia-Iliokastro seems to be developed.

The magmatic underpinning of Argolis Peninsula is corroborated by the results of a magnetotelluric study conducted by Galanopoulos et al (2005). These indicate upwelling of partially molten material not only at the Sousaki volcanic center where apparently it reached the surface, but also onshore, at the NW tip of Argolikos Gulf, near the city of Argos. Therein, the hot material is present at approx. 150 km depth, at the imaginary continuation of the long axis of the mid-crustal plutons detected beneath Argolikos Gulf. This might actually be the continuity of the deep hot-material that somehow is present in Argolikos Gulf at relatively shallower depths. Finally the presence of a thermal spring with temperatures 20-40 °C at Ermioni region and the average heat flow density calculated at 50-70 mW/m² (IGME, 2001) may indicate the existence of a potential

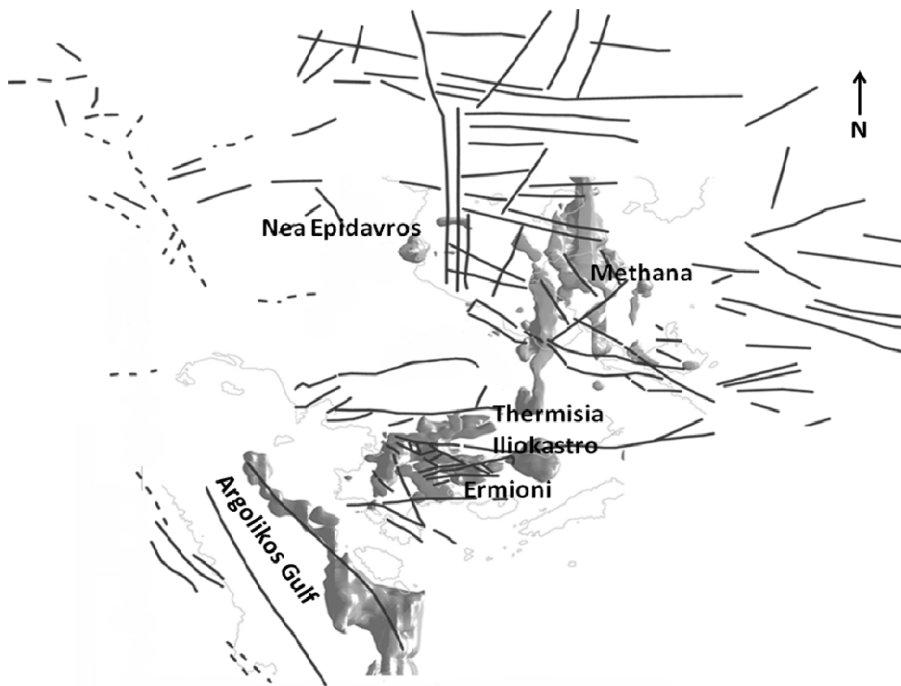


Figure 9: The tectonic grain of the study superimposed on the 0.02 isometric surface.

geothermal system. The geotectonic environment of magmatic volumes (probably plutons) which are present at considerable depths indicate rather an HDR (Hot Dry Rock) geothermal system commonly present at the peripheries of recent magmatic intrusions.

5. CONCLUSIONS

The inversion of the aeromagnetic data revealed a rather complex geological structure in terms of magnetic susceptibility. Scattered, relatively shallow (< 2km) and northerly dipping formations of ultramafic rocks have been identified at North and Central Argolis and ophiolitic lenses at South Argolis (depth < 500 m). On the contrary massive magnetized domains which are interpreted to be plutonites are present at mid-crustal depths (8 km) beneath the broader area of Argolis Peninsula.

The extensive and pervasive magmatic activity is evident in the widespread continuous presence of shallow and mid-crustal intrusions beneath Argolis peninsula and Saronikos Gulf. Particular attention should be given to one such elongate and deep reaching intrusion (pluton), which develops in a NNW direction (approx. 330°) along the axis of Argolikos Gulf, to the south of Argolis peninsula; this is situated almost directly above the local inflection (steepening) of the subducting slab and is almost exactly aligned with to it. The presence of this feature may be related to the subduction beneath the Peloponnese and to the stress transferred to the crust by the corresponding change in its dynamics; this will be the subject of future, rigorous investigation. Moreover, because the interaction of the subcrustal and crustal stress field results in a complex segmentation of the crust, their coupling also appears to facilitate and control the widespread and pervasive plutonic and volcanic magmatism of the study area and Argolis in particular.

Finally the presence of a thermal spring with temperatures 20-40 °C at Ermioni and the average heat flow density calculated at 50-70 mW/m² (IGME, 2001) indicate that hot dry rock may underlie the South Argolis Peninsula and Argolikos Gulf. This might represent a hidden geothermal system; this, however will also be the topic for future more rigorous investigation.

REFERENCES

- Anastasakis G., Piper D., Dermitzakis M., Karakitsios V., (2005) Upper Cenozoic stratigraphy and paleogeographic evolution of Myrtoon and adjacent basins, Aegean Sea, Greece. *Marine and Petroleum Geology* 23 (2006) 353–369.
- Billiris H., Paradissis D., Veis G., England P., Featherstone W., Parsons B., Cross P., Rands P., Rayson M., Sellers P., Ashkenazi V., Davison M., Jackson J., Ambrseys N., (1991), Geodetic determination of tectonic deformation in central Greece from 1900 to 1988. *Nature* 350:124-129.
- Briole P., Rigo A., Lyon-Caen H., Ruegg J.C., Papazissi K., Mitsakaki C., Balodimou A., Veis G., Hatzfeldand D., and Deschamps A., (2000), Active deformation of the Corinth Rift, Greece: results from repeated Global Positioning Systems surveys between 1990 and 1995. *J. Geophys. Res.*,105:25605 –25625.
- Brooks and Ferentinos (1984), Tectonics and sedimentology in the Gulf of Corinth and Zakynthos and Kefallinia channels, western Greece. *Tectonoph.* 101, p. 25-54
- Chailas S., Tzanis A., Kranis H., Karmis P., (2010), Compilation of a unified and homogeneous aeromagnetic map of the Greek Mainland. *Bulletin of the Geological Society of Greece*, 2010. Proceedings of the 12th International Congress, Patras, May.
- DeMartini, P.M., Pantosti, D., Palyvos, N., Lemeille, F., McNeill, L., and Collier, R., (2004), Slip rates of the Aigion and Eliki faults from uplifted marine terraces, Corinth Gulf, Greece: *Comptes Rendus Geoscience*, v. 336, p. 325– 334, doi: 10.1016/j.crte.2003.12.006.
- Drakatos G., Karastathis V, Makris J, Papoulia J, Stavrakakis G., 2005. 3D crustal structure in the neotectonic basin of the Gulf of Saronikos (Greece), *Tectonophysics*, 400, 55-65.
- Efstathiou A., Tzanis A., Chailas S., Stamatakis M., (2012), Imaging of the Methana Volcanic Complex, Greece , with magnetotelluric & aeromagnetic data. *EGU General Assembly, Vienna, Austria, 22-28 April 2012* (poster session: http://presentations.copernicus.org/EGU2012-11673_presentation.pdf).
- Gaitanakis P. and Photiades A. (1989), *Les Unites Ophiolitiques de l' Argolide (Peloponnese,Greece)*. *Bull. Geol. Soc. Greece*, XXIII /1, 363-380, Athens.
- Galanopoulos D., SakkaS V., Kosmatos D., Lagios E., (2005) Geoelectric investigation of the Hellenic subduction zone using long period magnetotelluric data. *Tectonophysics* 409, 73–84.
- Hatzfeld, D., Besnard M., Makropoulos K. and Hatzidimitriou P., 1993. Microearthquake seismicity and fault plane solutions in the southern Aegean and its geodynamic implications. *Geophys. J. Int.*, 115, 799-818.
- Hatzfeld D., Pedotti G., Hatzidimitriou P., et al (1989), The Hellenic subduction beneath the Peloponnesus: first results of a microearthquake study. *Earth and Planetary Sciences Letters*.93. 283-291
- Kiratzi A. and Louvari E., (2003), Focal mechanisms of shallow earthquakes in the Aegean Sea and the surrounding lands determined by waveform modelling: a new database. *Journal of Geodynamics*, 36, 251–274.
- Li Y. and Oldenburg D.W., (1996), 3-D inversion of magnetic data: *Geophysics* v.61, p.394-408.
- Li Y. and Oldenburg D.W., (1998), 3-D inversion of gravity data: *Geophysics* v.63, p.109-119.
- McNeill, L. C., Cotterill, C. J. et al. 2005. Active faulting within the offshore western Gulf of Corinth, Greece: implications for models of continental rift deformation. *Geology*, 33, 241–244, doi: 10.1130/G21127.1.
- Moretti, I., Sakellariou, D., Lykousis, V. and Micarelli, L. 2003. The Gulf of Corinth: an active half graben? *J. Geodyn.*, 36, 323–340.
- Nomikou P. and Papanikolaou D., (2010), Extension of active fault zones on Nisyros volcano across the Yali-Nisyros Channel based on onshore and offshore data. *Mar Geophys Res* (2011) 32:181–192. DOI 10.1007/s11001-011-9119z.
- Papanikolaou D., Lykousis V., Chronis G., Pavlakis P (1988), A comparative study of neotectonic basins a cross the Hellenic Arc: the Messiniakos, Argolikos, Saronikos and Southern Evoikos Gulfs. *Basin Research* 1, 167-176.
- Papanikolaou D. and Lozios S., (1990, 1991),
- Pe-Piper G. Pe. and Piper D.J.W, (2005), The South Aegean active volcanic arc: relationships between magmatism and tectonics.
- Ritsema, A., 1974. The earthquake mechanics of the Balkan region. *R. Netherl. Meteorol. Inst., De Bilt, Sci. Rep* 4–74.
- Rontogianni S., Konstantinou K. I, Melis N. S., and. Evangelidis C. P (2011) Slab stress field in the Hellenic subduction zone as inferred from intermediate-depth earthquakes. *Earth Plan. Sci. Let.*, 63, 139–144, 2011.
- Sachpazi, M., Clement, C., Laigle, M., Hirn, A. and Roussos, N. 2003. Rift structure, evolution, and earthquakes in the Gulf of Corinth, from reflection seismic images. *Earth Plan. Sci. Let.*, 216, 243-257.
- Scaillet A., Pichavant M., Cioni R., (2008), Upward migration of Vesuvius magma chamber over the past 20,000 years. *Nature* 455, 216-219.
- Stefatos, A., Papatheodorou, G., Ferentinos, G., Leeder, M. and COLLIER, R. 2002. Seismic reflection imaging of active offshore faults in the Gulf of Corinth: their seismotectonic significance. *Basin Research*, 14, 439-542.
- Suckale J., Rondenay. S, Sachpazi M, Charalampakis M., Hosa A and Royden L. H. (2009), High-resolution seismic imaging of the western Hellenic subduction zone using teleseismic scattered waves. *Geophys. J. Int.* (2009) 178, 775–791.
- Taktikos, St. et al. (2001), Map of Heat Flow Density in Greece, 1:1000000 scale. Institute of Geology and Mineral Exploration (IGME), Athens, Greece